Atomic structure of As_2S_3–Ag chalcogenide glasses

Atomic structure of As_2S_3–Ag chalcogenide glasses

I Kaban[1]**, P Jóvári**[2]**, T Wagner**[3,4]**, M Frumar**[3]**, S Stehlik**[3]**,
M Bartos**[3]**, W Hoyer**[1]**, B Beuneu**[5] **and M A Webb**[6]

[1] Institute of Physics, Chemnitz University of Technology, D-09107 Chemnitz, Germany
[2] Research Institute for Solid State Physics and Optics, H-1525 Budapest, POB 49, Hungary
[3] Faculty of Chemical Technology, University of Pardubice, Čs. legií 565 square,
532 10 Pardubice, Czech Republic
[4] Centre for Material Science, University of Pardubice, Studentská 95, 53002 Pardubice,
Czech Republic
[5] Laboratoire Léon Brillouin, CEA-Saclay, 91191 Gif sur Yvette Cedex, France
[6] Hamburger Synchrotronstrahlungslabor HASYLAB am Deutschen Elektronen-Synchroton
DESY, Notkestrasse 85, D-22603 Hamburg, Germany

E-mail: ivan.kaban@physik.tu-chemnitz.de

Abstract

$(As_{0.4}S_{0.6})_{100-x}Ag_x$ glasses ($x = 0$, 4, 8, 12 at.%) have been studied with high-energy x-ray
diffraction, neutron diffraction and extended x-ray absorption spectroscopy at As and Ag
K-edges. The experimental data were modelled simultaneously with the reverse Monte Carlo
simulation method. Analysis of the partial pair correlation functions and coordination numbers
extracted from the model atomic configurations revealed that silver preferentially bonds to
sulfur in the As_2S_3–Ag ternary glasses, which results in the formation of homoatomic As–As
bonds. Upon the addition of Ag, a small proportion of Ag–As bonds ($N_{AgAs} \approx 0.3$) are formed
in all three ternary compositions, while the direct Ag–Ag bonds ($N_{AgAg} \approx 0.4$) appear only in
the glass with the highest Ag content (12 at.%). Similar to the g-As_2S_3 binary, the mean
coordination number of arsenic is close to three, and that of sulfur is close to two, in the
As_2S_3–Ag ternary glasses. The first sharp diffraction peak on the total structure factors of As_2S_3
binary and $(As_{0.4}S_{0.6})_{100-x}Ag_x$ ternary glasses is related to the As–As and As–S correlations.

(Some figures in this article are in colour only in the electronic version)

1. Introduction

Amorphous chalcogenides are known for their unique properties such as electric switching, reversible amorphous-to-crystalline transition or high infrared transmittance. Technologies based on chalcogenide glasses are applied successfully in phase change optical recording or optical telecommunications, for example. The interest in As–S and As–Se chalcogenide glasses with additions of Ag is due to their ionic conductivity [1–6]. As–S–Ag alloys have been investigated in relation to possible practical applications in different technological processes or devices such as lithography [7], diffractive optical gratings [8], information storage devices [9], optical switches [10], and sensitive electrochemical electrodes [11]. The interest stems from the fact that the physical properties

of glasses are tightly related to their structure; a profound knowledge of the latter can help to understand these materials better, improve their physical properties, and exploit them more efficiently.

Maruno *et al* [2] studied the electrical properties of As_2S_3–Ag glasses and suggested that Ag atoms are presumably joined to S atoms by ionic bonds. Ohta [4] explained the change of electrical conduction in As_2S_3 glasses doped with Ag by the breaking of As–S–As links and formation of Ag–S and As–As bonds. Mastelaro *et al* [12] performed an extended x-ray absorption fine structure (EXAFS) study of the ternary glasses along the pseudo-binary line (Ag_2S)–(As_2S_3). They found that each As atom is coordinated by three S atoms ($r_{AsS} = 2.25$–2.27 Å) and Ag is coordinated by two S atoms ($r_{AgS} = 2.46$–2.48 Å) at any Ag concentration. However, proceeding from

Table 1. Mass density of $(As_{0.4}S_{0.6})_{100-x}Ag_x$ glasses measured by the Archimedean method and the number density calculated.

Alloy	Mass density (g cm^{-3})	Number density (atoms Å^{-3})
As$_2$S$_3$	3.185 ± 0.005	0.0390
(As$_{0.4}$S$_{0.6}$)$_{96}$Ag$_4$	3.465 ± 0.005	0.0405
(As$_{0.4}$S$_{0.6}$)$_{92}$Ag$_8$	3.675 ± 0.006	0.0412
(As$_{0.4}$S$_{0.6}$)$_{88}$Ag$_{12}$	3.893 ± 0.006	0.0417

the fact that the glasses are based on stoichiometric As$_2$S$_3$, they excluded homoatomic As–As bonding in ternary glasses. Penfold and Salmon [13] studied two glasses As$_{37.6}$S$_{58.4}$Ag$_4$ and As$_{25}$S$_{50}$Ag$_{25}$ with neutron diffraction (ND) using ^{107}Ag and ^{109}Ag isotopes. They established that (i) As remains three-fold coordinated by S atoms both at low and high concentrations of Ag; (ii) Ag is four-fold coordinated in the As$_{37.6}$S$_{58.4}$Ag$_4$ glass and is three-fold coordinated in the As$_{25}$S$_{50}$Ag$_{25}$ glass. A small proportion of Ag–Ag correlations at distances around 2.97 Å was found, but neither As–As nor Ag–As bonds were identified. Bychkov and Price [14] investigated (Ag$_2$S)–(As$_2$S$_3$) containing up to 25 at.% Ag with neutron diffraction. They separated As–S, Ag–S and Ag–Ag correlations by multi-peak Gaussian fitting of the total radial distribution functions. Ag–Ag correlations were not found in the glasses with a low Ag content (4 at.%), but they appeared at about 3 Å ($N_{AgAg} \approx 1$) in the glasses with a Ag concentration larger than 10–15 at.%.

In this work we perform a complex structural study of glassy (*g*-) $(As_{0.4}S_{0.6})_{100-x}Ag_x$ alloys ($x = 0, 4, 8, 12$ at.%) using x-ray diffraction (XRD), neutron diffraction and EXAFS experimental techniques and a reverse Monte Carlo (RMC) simulation method. Simultaneous modelling of several experimental datasets for each composition enables one to obtain the partial pair distribution functions and to extract the information on the local atomic distribution in the glasses. In section 2, we describe the details of the sample preparation and experiments, and present the data obtained. The RMC modelling is recalled in section 3. The general experimental observations as well as the results of RMC modelling are analysed in section 4. Our findings are summarized in section 5.

2. Experimental details and results

$(As_{0.4}S_{0.6})_{100-x}Ag_x$ bulk glasses ($x = 0, 4, 8, 12$ at.%) were prepared from Ag, As and S of 5N purity. Pure elements were weighed in the required molar ratio and sealed in silica ampoules under a residual pressure $\approx 10^{-4}$ Pa. The atomic As was purified by sublimation to avoid oxide formation just before weighing. The sealed ampoules were put into a rocking furnace and held at 750 °C for 24 h. The bulk samples were quenched in air and annealed at 120 °C for 3 h. The samples were kept under inert atmosphere of N$_2$ after breaking the synthesis ampoules.

The mass density of the alloys was determined with an accuracy of $\pm 0.15\%$ using the Archimedean method by
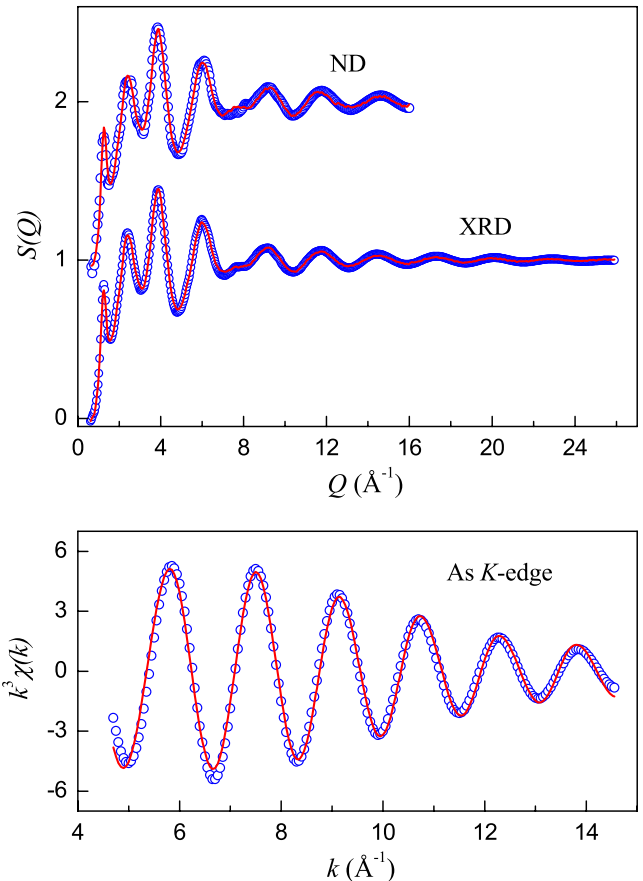

Figure 1. XRD and ND structure factors, and As K-adsorption edge EXAFS for As$_2$S$_3$ glass: *circles*—measurement; *lines*—data obtained by simultaneous RMC simulation of the experimental XRD, ND data without As–As and S–S bonding.

weighing samples in air and in toluene. The densities are listed in table 1.

All compositions were studied with x-ray diffraction at the BW5 experimental station at HASYLAB (DESY, Hamburg) [15]. Bulk samples of about 2 mm thickness were examined in a transmission geometry. The energy of the incident beam was 99.8 keV and the beam size was 1 × 4 mm^2. The scattered intensity was recorded by a Ge solid-state detector. The raw data were corrected for background, absorption, polarization, detector dead-time and variations in detector solid angle [16].

The EXAFS measurements were carried out for all compositions at the Ag and As K-absorption edges at the X1 experimental station at HASYLAB [15] in transmission mode. The samples were finely ground, mixed with cellulose and pressed into tablets. The sample quantity in the tablets was adjusted for the composition of the sample and to the selected edge to achieve an approximate transmission of $1/e$. EXAFS spectra were obtained with steps of 0.5 eV near the absorption edge. The measuring time was k-weighted during the collection of the signal. The x-ray absorption cross sections $\mu(E)$ were converted to $\chi(k)$ by standard procedures of data reduction using the program Viper [17].

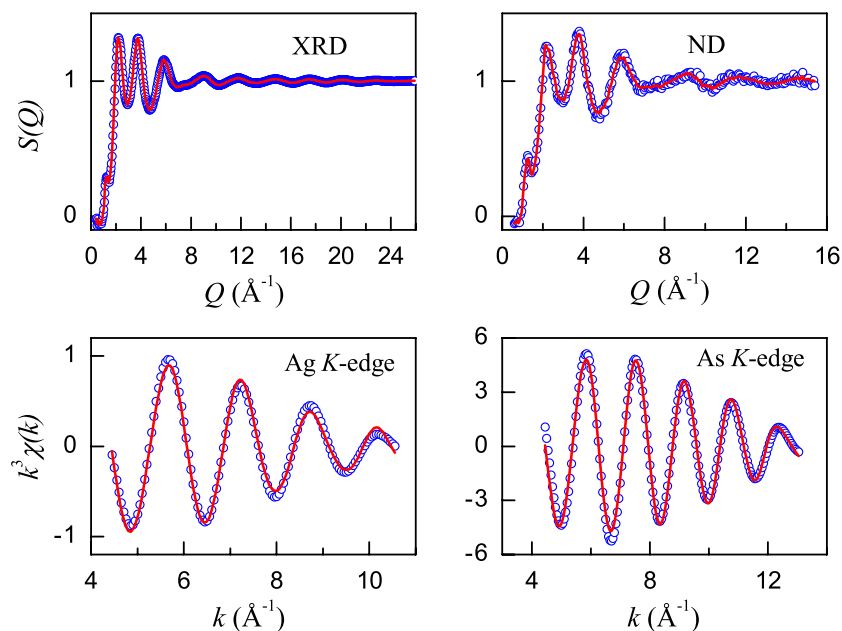The neutron diffraction experiment was carried out for As$_2$S$_3$ and (As$_{0.4}$S$_{0.6}$)$_{88}$Ag$_{12}$ glasses with the 7C2

Figure 2. XRD and ND structure factors, and EXAFS spectra for $(As_{0.4}S_{0.6})_{88}Ag_{12}$ glass: *circles*—measurement; *lines*—data obtained by simultaneous RMC simulation of the experimental XRD, ND and EXAFS data without S–S bonding. The coordination number for As atoms was constrained to be 3.

diffractometer at the Léon Brillouin Laboratory (CEA-Saclay, France). The samples were filled into thin walled (0.1 mm) vanadium containers of 5 mm diameter. The raw data were corrected for detector efficiency, empty instrument background, scattering from the sample holder, multiple scattering, and absorption.

Figures 1 and 2 show the whole sets of the experimental data—XRD, ND and EXAFS—for the binary As_2S_3 and ternary $(As_{0.4}S_{0.6})_{88}Ag_{12}$ glasses. The experimental structure factors obtained with XRD and the corresponding pair distribution functions for all $(As_{0.4}S_{0.6})_{100-x}Ag_x$ glasses studied are compared in figure 3.

3. Reverse Monte Carlo modelling

Reverse Monte Carlo modelling enables the construction of large three-dimensional structural models compatible with available experimental information. Partial pair distribution functions, most probable interatomic distances and coordination numbers can be extracted from the model atomic configuration. The details of RMC and its application to chalcogenide glasses can be found elsewhere [18–22].

In the present work, the atomic structures of the As_2S_3 binary glass and $(As_{0.4}S_{0.6})_{100-x}Ag_x$ ternary glasses have been modelled with the new RMCPP code [23]. The simulation boxes contained 20000 atoms. The number densities ρ used in the simulations were calculated from the mass densities given in table 1. The choice of proper minimum interatomic distances (cut offs) is essential: too high values may prevent RMC from achieving a good fit, while too low cut offs may result in the mixing of originally non-overlapping peaks. RMC tends to produce the most disordered atomic configuration compatible with experimental data. Thus, in a multicomponent

Table 2. Minimum interatomic distances (cut offs) applied in the RMC simulation of $(As_{0.4}S_{0.6})_{100-x}Ag_x$ glasses.

Pair	As–As	As–S	As–Ag	S–S	S–Ag	Ag–Ag
Cut off (Å)	2.3	1.9	2.3	2.7	2.4	2.6

system the presence/absence of some characteristic interatomic distances (bonds) is not necessarily revealed by a single simulation run. For this reason several test runs were carried out with varying cut offs. For all compositions satisfactory fits of experimental data could be achieved by applying a minimum S–S distance as high as 2.7 Å. The choice of As–Ag and Ag–Ag minimum distances will be discussed below. Cut offs applied in the 'final' runs (used to produce configurations for further analysis) are listed in table 2.

The backscattering amplitudes needed to obtain the model EXAFS curves from the pair distribution functions were calculated by the FEFF8.4 program [24]. As an example, fits obtained by simultaneous modelling of all available independent measurements for As_2S_3 binary and $(As_{0.4}S_{0.6})_{88}Ag_{12}$ ternary glasses are compared with the experimental data in figures 1 and 2. Similar good quality fits were obtained for the alloys with 4 and 8 at.% Ag (not shown). Partial pair distribution functions $g_{ij}(r)$ corresponding to the model configurations for all compositions studied are shown in figure 4. The corresponding mean nearest neighbour distances r_{ij} and coordination numbers N_{ij} are presented in table 3. It should be noted that only neighbours within the first coordination shell are considered. The uncertainty of r_{ij} is usually around ± 0.02 Å, but it can be significantly higher (0.05–0.1 Å) for atomic pairs with a low contribution to the total pair distribution function. The error of the mean
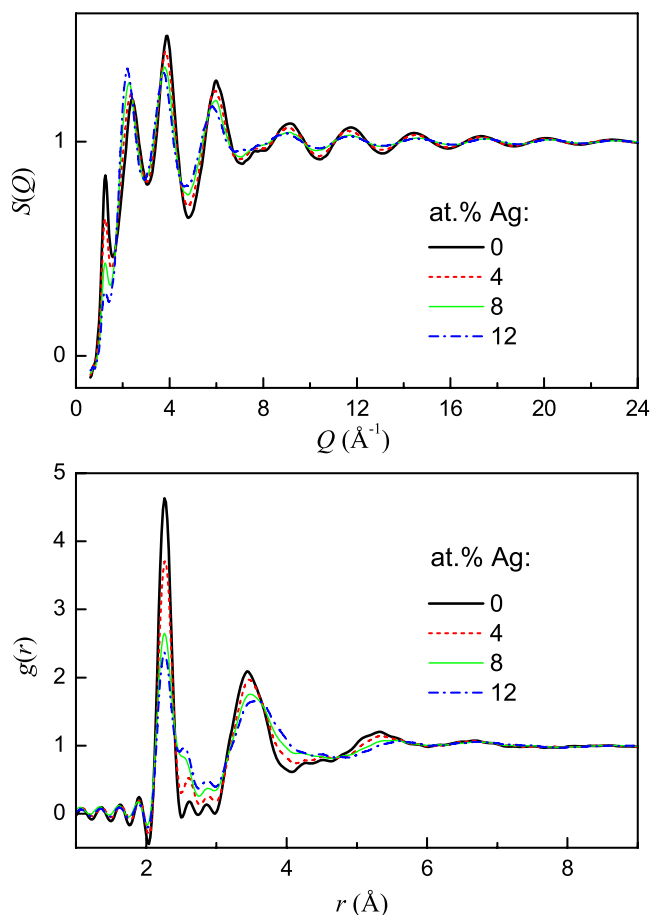
Figure 3. XRD total structure factors $S(Q)$ and pair distribution functions $g(r)$ for $(As_{0.4}S_{0.6})_{100-x}Ag_x$ glasses.

coordination number for alloy constituents N_{iX} is around 5–10%, while that of partial coordination numbers N_{ij} can again be higher, especially for low concentration alloy constituents. The absolute uncertainty of these values is about ± 0.2.

4. Discussion

4.1. General observations

Crystalline As_2S_3 (orpiment) has a monoclinic structure with eight As atoms and twelve S atoms in the unit cell [25]. Each As atom is covalently bonded to three S atoms in a pyramidal unit and each S atom is bonded to two As atoms. Covalently bonded $AsS_{3/2}$ units form layers parallel to the *a–c* plane, which are weakly connected by van der Waals forces along the *b* axis. The mean As–S distance is 2.24 Å, that of As–As is 3.48 Å and that of S–S is 3.40 Å.

The structure of As_2S_3 glass is usually presented as a random network of layers composed of $AsS_{3/2}$ pyramidal units, which are linked together by corner-sharing sulfur atoms. The layers are held together through weak intermolecular forces like that in the crystalline state. For example, Iwadate *et al* [26] studied As_2S_3 glass with XRD and ND. They established that each As atom has approximately three S nearest neighbours at the distance of 2.27 Å and the closest approach distances for

the homoatomic pairs As–As and S–S are 3.48 Å and 3.32 Å respectively. These values are very close to those found in orpiment.

Structural changes in the $(As_{0.4}S_{0.6})_{100-x}Ag_x$ glasses with increasing Ag content can already be revealed by analysis of the x-ray diffraction structure factors and pair distribution functions (figure 3). The intensity of the first sharp diffraction peak (FSDP) on the experimental $S(Q)$s is decreases remarkably, while its position at about 1.26 Å^{-1} remains constant. The second maximum shifts to smaller values of the diffraction vector Q—from 2.41 Å^{-1} for $x = 0$ to 2.19 Å^{-1} for $x = 12$. The next maxima shift to higher Q-values and the intensity of oscillations decreases with increasing Ag concentration.

The peak of the $g(r)$ functions at $r = 2.26$ Å reflects the As–S bonding. This value (2.26 Å) is close to the mean As–S distance in crystalline As_2S_3 [25] as well as to the sum of covalent radii for As and S [27]. The intensity of this peak decreases continuously with increasing Ag concentration. At the same time, a shoulder on the $g(r)$ at 2.5–2.6 Å appears for the alloys with 4 and 8 at.% Ag, and it develops into a peak at 12 at.% Ag. This distance correlates with the sum of covalent radii for Ag and S (2.50–2.58 Å [27]). Based on these observations, it can be concluded that the number of As–S pairs decreases and Ag–S bonds appear in the ternary glasses when Ag is alloyed with As_2S_3. If we suppose that As remains three-fold coordinated, then it is reasonable to assume that the reduction of the number of As–S pairs is compensated by the formation of 'wrong' As–As pairs. However this cannot be proven directly from the total structure factors or pair distribution functions of ternary alloys because the As–As contribution to the diffraction curve would be covered by the intense As–S scattering. Therefore, analysis on the level of partial atomic distributions and coordination numbers is required.

4.2. Analysis of the RMC models

Bearing in mind that the formation of homoatomic As–As bonds is very probable in the $(As_{0.4}S_{0.6})_{100-x}Ag_x$ ternary glasses, we checked the sensitivity of RMC models to these correlations. For this, the existence of As–As bonding in the As_2S_3 binary glass was tested. At first, the XRD and ND structure factors of g-As_2S_3 were modelled with the cut offs prohibiting direct As–As and S–S bonds: $r_{AsAs}^{min} = 2.9$ Å, $r_{AsS}^{min} = 1.9$ Å, $r_{SS}^{min} = 2.7$ Å. The model curves excellently coincide with those obtained in the experiments as it is seen in figure 1. The mean coordination numbers extracted from the model partial pair distribution functions ($N_{AsS} = 2.94$ and $N_{SAs} = 1.96$) correspond to the valences of As and S. The quality of the RMC fit was also very good if the As–As cut off was decreased to 2.3 Å, that is, when direct As–As bonds were allowed. In this case, $N_{AsAs} = 0.2$, $N_{AsS} = 2.76$, and $N_{SAs} = 1.84$ were obtained. Hence, as it follows from our modelling, there might be a small proportion of homoatomic As–As bonds in the glassy As_2S_3. However, the above value of N_{AsAs} is close to the error of the model.
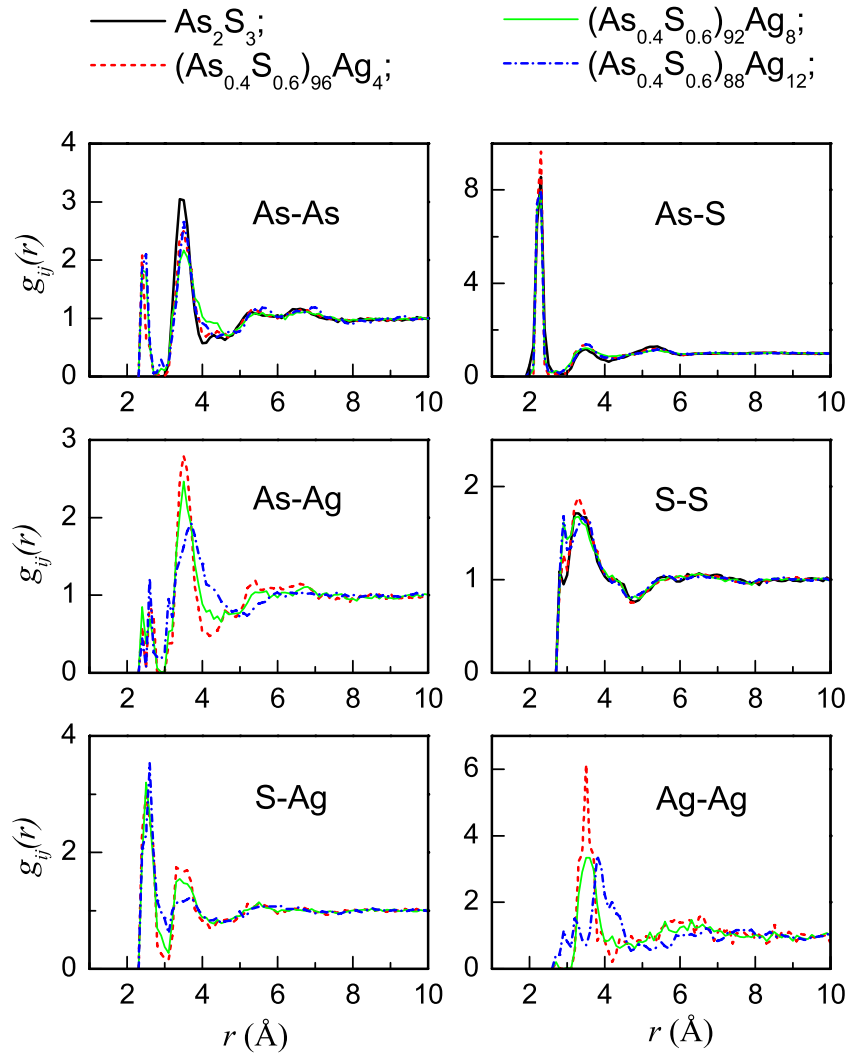
Figure 4. Partial pair distribution functions for $(As_{0.4}S_{0.6})_{100-x}Ag_x$ glasses obtained with RMC. The coordination number for As atoms was constrained to be 3. Direct S–S bonds were forbidden in all models. The values presented for As_2S_3 composition are extracted from the model without homoatomic As–As and S–S bonds.

Table 3. The nearest neighbour distances r_{ij} (within the first coordination shell) and coordination numbers N_{ij} for $(As_{0.4}S_{0.6})_{100-x}Ag_x$ glasses obtained with RMC modelling. The coordination number for As atoms was constrained to be 3. Direct S–S bonds were forbidden in all models. The values presented for As_2S_3 composition are extracted from the model where homoatomic As–As and S–S bonds were forbidden.

Pairs, $i-j$	As_2S_3 r_{ij} (Å)	N_{ij}	$As_{38.4}S_{57.6}Ag_4$ r_{ij} (Å)	N_{ij}	$As_{36.8}S_{55.2}Ag_8$ r_{ij} (Å)	N_{ij}	$As_{35.2}S_{52.8}Ag_{12}$ r_{ij} (Å)	N_{ij}
As–As	—	—	2.44	0.4	2.46	0.49	2.47	0.53
As–S/S–As	2.26	2.94/1.96	2.26	2.68/1.79	2.26	2.42/1.61	2.26	2.39/1.59
As–Ag/Ag–As	—	—	2.64	0.03/0.29	2.60	0.06/0.29	2.60	0.09/0.28
Ag–Ag	—	—	—	0	—	0	2.9–3.2	0.39
Ag–S/S–Ag	—	—	2.54	2.15/0.15	2.56	2.11/0.31	2.58	2.55/0.58
S–S	—	0	—	0	—	0	—	0
As–X	—	2.94	—	3.11	—	2.97	—	3.01
S–X	—	1.96	—	1.94	—	1.92	—	2.17
Ag–X	—	—	—	2.44	—	2.41	—	3.22

Taking into account the coordination numbers obtained for g-As_2S_3 and the results of previous studies on ternary As–S–Ag glasses (EXAFS [12], ND [13]), the coordination constraint $N_{AsX} = 3$ was applied in the modelling of ternary glasses. That is, for each As atom the sum of nearest neighbours (regardless the type) had to be 3. In the final configurations 90–95% of As atoms satisfied the above condition. From preliminary (unconstrained) runs it had been already clear that Ag bonds mostly to S. To see how the coordination number of S changes upon adding Ag, the coordination number
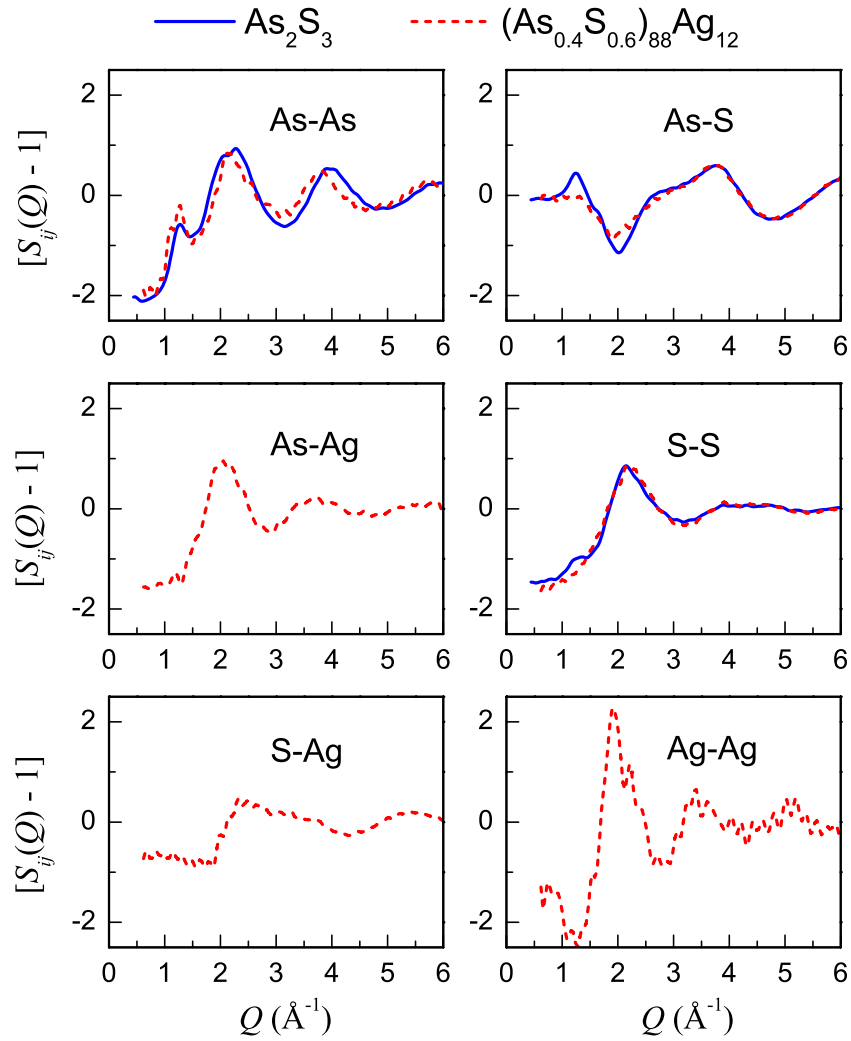
Figure 5. Reduced partial structure factors $[S_{ij}(Q) - 1]$ for g-As$_2$S$_3$ (*solid lines*) and g-(As$_{0.4}$S$_{0.6}$)$_{88}$Ag$_{12}$ (*dashed lines*).

of sulfur *was not* constrained (this is why we can say that $N_S = 2$ comes from the data and not from the constraints). Direct S–S bonds were considered as very improbable in the ternary glasses (As$_{0.4}$S$_{0.6}$)$_{100-x}$Ag$_x$ and were therefore forbidden during modelling. The results of constrained RMC simulations confirm that Ag is predominantly bonded to S atoms when it is added to the As$_2$S$_3$ binary. The number of S–As nearest neighbours gradually decreases from 2 in g-As$_2$S$_3$ to about 1.6 in As$_{35.2}$S$_{52.8}$Ag$_{12}$ glass. The mean coordination number N_{AsAs} in the ternary glasses is larger (0.4–0.5) than that obtained for the As$_2$S$_3$ binary (0.2), which suggests that 'wrong' As–As bonds ($r_{AsAs} = 2.46$–2.47 Å) are already formed upon addition of 4 at.% Ag.

Better RMC fits were obtained when Ag–As bonds were allowed in the ternary glasses. A small peak appeared on the $g_{AsAg}(r)$ with the maximum at 2.6 Å, which correlates with the sum of Ag and As covalent radii. It is interesting that for all ternary compositions, one Ag atoms has on average approximately 0.3 As nearest neighbours.

If the Ag–Ag bonds are allowed in the ternary models, there appear two small peaks on the $g_{AgAg}(r)$ for the As$_{35.2}$S$_{52.8}$Ag$_{12}$ composition—one at 2.9 Å and another at

3.2 Å. Integration over these two peaks yields $N_{AgAg} \approx 0.4$. It is worth noting that no direct Ag–Ag contacts are formed in the model structures for g-As$_{38.4}$S$_{57.6}$Ag$_4$ and g-As$_{36.8}$S$_{55.2}$Ag$_8$. The closest approach between Ag atoms in these two glasses is about 3.5 Å.

A remarkable feature of the total XRD and ND structure factors for g-As$_2$S$_3$ binary (figure 1) is the first sharp diffraction peak at about 1.26 Å^{-1}, whose intensity decreases upon addition of Ag (figures 2 and 3). Zhou *et al* [28] studied glassy As$_2$S$_3$ with the help of anomalous x-ray diffraction and concluded that the FSDP is mainly caused by As–As correlations extended as far as 7 Å [28]. Bychkov and Price [14], who observed the reduction of FSDP in the (Ag$_2$S)–(As$_2$S$_3$), suggested that this is related to the transformation and fragmentation of the As$_2$S$_3$ network with increasing Ag concentration.

The nature of the FSDP can be revealed by analysis of the partial structure factors $S_{ij}(Q)$ related to the respective pair distribution functions $g_{ij}(r)$ via the Fourier transformation:

$$S_{ij}(Q) = 1 + \frac{4\pi\rho_0}{Q} \int r \sin Qr (g_{ij}(r) - 1)\, \mathrm{d}r, \quad (1)$$
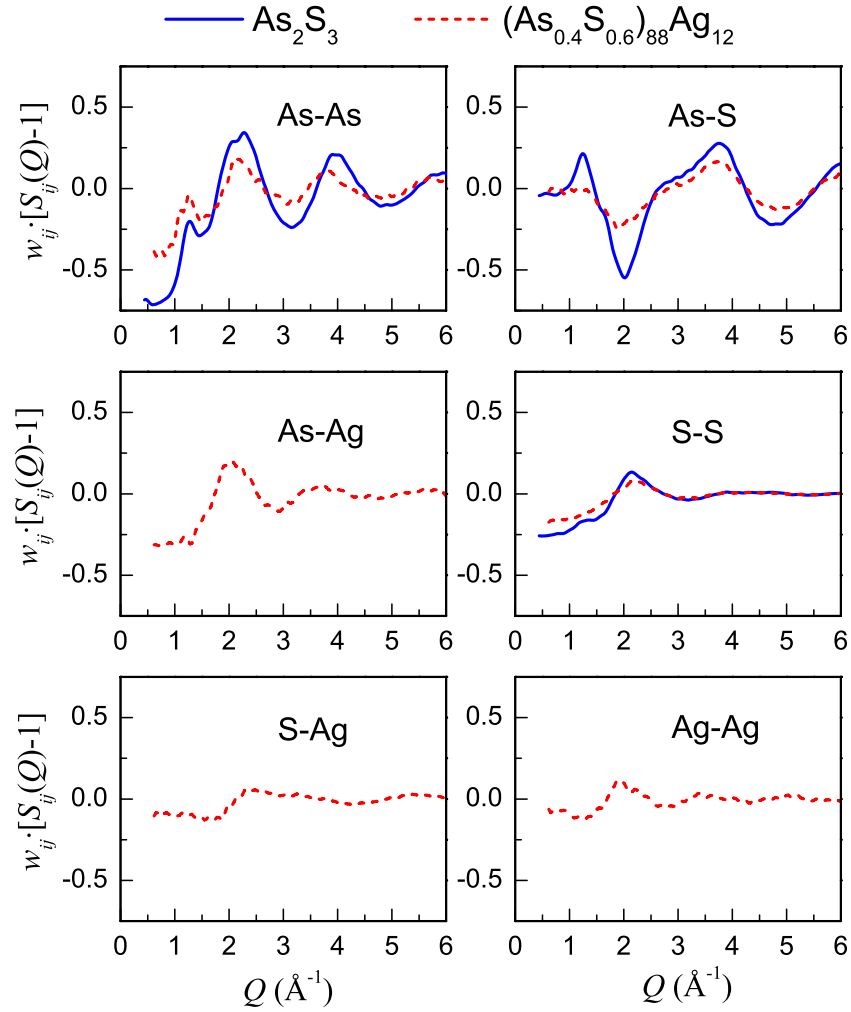
Figure 6. Weighted reduced XRD partial structure factors $w_{ij}[S_{ij}(Q) - 1]$ for g-As$_2$S$_3$ (*solid lines*) and g-(As$_{0.4}$S$_{0.6}$)$_{88}$Ag$_{12}$ (*dashed lines*).

Table 4. XRD weighting coefficients w_{ijs} for (As$_{0.4}$S$_{0.6}$)$_{100-x}$Ag$_x$ glasses at $Q = 0$.

w_{ijs}	As$_2$S$_3$	As$_{38.4}$S$_{57.6}$Ag$_4$	As$_{36.8}$S$_{55.2}$Ag$_8$	As$_{35.2}$S$_{52.8}$Ag$_{12}$
w_{AsAs}	0.335	0.284	0.241	0.204
w_{AsS}	0.488	0.413	0.351	0.297
w_{AsAg}	—	0.084	0.149	0.198
w_{AgAg}	—	0.006	0.023	0.048
w_{AgS}	—	0.061	0.109	0.144
w_{SS}	0.177	0.150	0.127	0.108

where $Q = 4\pi \sin\theta/\lambda$ is the magnitude of the diffraction vector, λ is the radiation wavelength, 2θ is the diffraction angle, and ρ_0 is the mean atomic number density. Figure 5 shows the reduced partial structure factors $[S_{ij}(Q) - 1]$ for As$_2$S$_3$ and As$_{35.2}$S$_{52.8}$Ag$_{12}$ glasses obtained from the partial pair distribution functions plotted in figure 4. Strong first sharp diffraction peaks are seen at about 1.26 Å^{-1} on the $S_{AsAs}(Q)$ and $S_{AsS}(Q)$ functions of the g-As$_2$S$_3$ binary. With the addition of Ag, the intensity of the FSDP on $S_{AsAs}(Q)$ increases, while that of the FSDP on the $S_{AsS}(Q)$ function decreases. At the same time, the $S_{AgAg}(Q)$ curve has a deep minimum at ~1.26 Å^{-1}. To distinguish the contribution of

each atomic pair to the FSDP, it should be taken into account that the total structure factor $S(Q)$ is a weighted sum of the partial $S_{ij}(Q)$s:

$$S(Q) - 1 = \sum_{ij} w_{ij}(Q)[S_{ij}(Q) - 1]. \tag{2}$$

The weighting coefficients w_{ij} depend on alloy composition and on the type of radiation. For the x-ray diffraction, w_{ij} can be calculated from the concentrations c_i and atomic form factors f_i with the expression:

$$w_{ij}(Q) = \frac{(2 - \delta_{ij})c_i c_j f_i(Q) f_j(Q)}{\sum_{ij} c_i c_j f_i(Q) f_j(Q)}, \tag{3}$$

δ_{ij} is the Kronecker symbol. In the case of neutron diffraction the atomic form factors have to be replaced by the coherent neutron scattering lengths, which are Q-independent.

The XRD weights w_{ij} at $Q = 0$ for (As$_{0.4}$S$_{0.6}$)$_{100-x}$Ag$_x$ glasses are listed in table 4, while the weighted reduced partial structure factors $w_{ij}[S_{ij}(Q)-1]$ for As$_2$S$_3$ and As$_{35.2}$S$_{52.8}$Ag$_{12}$ glasses are plotted in figure 6. It is clearly seen that the FSDP at about 1.26 Å^{-1} on the total XRD structure factor of g-As$_2$S$_3$ is related to the As–As and As–S correlations. Upon addition

of Ag to the As_2S_3 binary, the number of As–S bonds decreases and As–As bonds are formed. This is reflected on the partial structure factors in decreasing intensity at $1.26 \, \text{Å}^{-1}$ for the As–S pairs and increasing intensity for the As–As pairs. However, the intensity of the FSDP on the XRD total structure factor decreases (figure 3). The decrease is explained by the fact that the increase of the As–As pairs (N_{AsAs}) is compensated by the decrease of their weight (w_{AsAs}) in the total structure factor, while for the As–S pairs both the coordination number (N_{AsS}) and the XRD weighting coefficient (w_{AsS}) decrease (tables 3 and 4). The slight increase of the intensity at low Q-values on the S–S partial structure factor is balanced by a minimum on the Ag–Ag partial structure factor (figure 6). Therefore, these correlations (Ag–Ag and S–S) have virtually no influence on the FSDP intensity of the total structure factor for $(As_{0.4}S_{0.6})_{100-x}Ag_x$ ternary glasses.

5. Conclusions

The results of the present study show that addition of Ag to As_2S_3 mainly results in the formation of Ag–S and As–As bonds. The average number of heteroatomic As–S bonds gradually decreases from 3 in the As_2S_3 glass to 2.4 in g-$As_{35.2}S_{52.8}Ag_{12}$. At the same time, homoatomic As–As bonds are formed; their number reaches 0.4–0.5 for the ternary glasses with 4, 8 and 12 at.% Ag. Upon the addition of Ag, a small proportion of Ag–As bonds is formed, which is the same ($N_{AgAs} \approx 0.3$) for all three ternary compositions, while the direct Ag–Ag bonds ($N_{AgAg} \approx 0.4$) appear only in the glass with highest Ag content (12 at.%). It is noteworthy that the addition of Ag does not change the mean coordination number of As and S. Similar to the g-As_2S_3 binary, the mean coordination number of arsenic is close to three and that of sulfur is close to two in the As_2S_3–Ag ternary glasses. It is shown that the first sharp diffraction peak on the total structure factors of As_2S_3 binary and $(As_{0.4}S_{0.6})_{100-x}Ag_x$ ternary glasses is related to the As–As and As–S correlations. The decrease of the FSDP intensity on the structure factors of the ternary glasses is explained in the first place by the reduction of the number of As–S bonds upon the addition of Ag to the As_2S_3 binary.

Acknowledgments

References

[1] Borisova Z U 1981 *Glassy Semiconductors* (New York: Plenum)
[2] Maruno S, Noda M, Kondo Y and Yamada T 1972 *Japan. J. Appl. Phys.* **11** 116
[3] Kotkata M F and Mohamed C S 1989 *J. Mater. Sci.* **24** 1291
[4] Ohta M 1997 *Phys. Status Solidi* a **159** 461
[5] Kitao M, Ishikawa T and Yamada S 1986 *J. Non-Cryst. Solids* **79** 205
[6] Zima V, Wágner T, Vlček M, Beneš L, Kasap S O and Frumar M 2003 *J. Non-Cryst. Solids* **326/327** 159
[7] Kovalskiy A, Jain H, Neilson J, Vlček M, Waits C M, Churaman W and Dubey M 2007 *J. Phys. Chem. Solids* **68** 920
[8] Orava J, Wágner T, Krbal M, Kohoutek T, Vlček M, Beneš L, Kotulanova E, Bezdicka P, Klapetek P and Frumar M 2007 *J. Phys. Chem. Solids* **68** 1008
[9] Kozicki M N and Mitkova M 2006 *J. Non-Cryst. Solids* **352** 567
[10] Hirose Y and Hirose H 1976 *J. Appl. Phys.* **47** 2767
[11] Mourzina Y, Yoshinobu T, Schubert J, Lüth H, Iwasaki H and Schönning M J 2001 *Sensors Actuators* B **80** 136
[12] Mastelaro V, Benazeth S and Dexpert H 1995 *J. Non-Cryst. Solids* **185** 274
[13] Penfold I T and Salmon P S 1990 *Phys. Rev. Lett.* **64** 2164
[14] Bychkov E and Price D L 2000 *Solid State Ion.* **136/137** 1041
[15] http://hasylab.de/
[16] Poulsen H F, Neumann H-B, Schneider J R, Neuefeind J and Zeidler M D 1995 *J. Non-Cryst. Solids* **188** 63
[17] Klementev K V 2001 *J. Phys. D: Appl. Phys.* **34** 209
[18] McGreevy R L 2001 *J. Phys.: Condens. Matter* **13** R877
[19] Evrard G and Pusztai L 2005 *J. Phys.: Condens. Matter* **17** S1
[20] Jóvári P, Kaban I, Steiner J, Beuneu B, Schöps A and Webb A 2007 *J. Phys.: Condens. Matter* **19** 335212
[21] Jóvári P, Kaban I, Steiner J, Beuneu B, Schöps A and Webb A 2008 *Phys. Rev.* B **77** 035202
[22] Jóvári P, Yannopoulos S N, Kaban I, Kalampounias A, Lishchynskyy I, Beuneu B, Kostadinova O, Welter E and Schöps A 2008 *J. Chem. Phys.* **129** 214502
[23] Gereben O, Jóvári P, Temleitner L and Pusztai L 2007 *J. Optoelectron. Adv. Mater.* **9** 3021
[24] Ankudinov A L, Ravel B, Rehr J J and Conradson S D 1998 *Phys. Rev.* B **58** 7565
[25] Mullen D J E and Nowacki W 1972 *Z. Kristallogr.* **136** 48
[26] Iwadate Y, Hattori T, Nishiyama S, Fukushima K, Mochizukia Y, Misawa M and Fukunaga T 1999 *J. Phys. Chem. Solids* **60** 1447
[27] www.webelements.com
[28] Zhou W, Sayers D E, Paesler M A, Boucher-Fabre B, Ma Q and Raoux D 1993 *Phys. Rev.* B **47** 686